A mathematical model toward quantitative assessment of parallel imaging reconstruction

Y. Li[1], F. Huang[1], W. Lin[1], and A. Reykowski[1]
[1]Advanced Concept Development, Invivo Diagnostic Imaging, Gainesville, Florida, United States

Introduction: Quantitative image quality assessment is an unresolved issue in MRI, especially for partially parallel imaging (PPI) [1, 2]. It follows that no clear definition can be made for the "optimization" of a reconstruction algorithm. This also makes it difficult to evaluate the design of a receive coil array for PPI. To tackle this issue, we propose a mathematical model to reduce the complexity of image quality assessment by separating the reconstruction error into three components, which affect image quality in different fashions because of their different patterns in image space. In this model, explicit representations are given for three types of errors in the reconstruction of Cartesian imaging data. These errors are distinguished as image fidelity error, residual aliasing artifacts, and amplified noise. Based on this model, practical techniques can be developed with the freedom to quantitatively adjust the relative significance of three types of errors in a reconstruction algorithm. By minimizing the weighted sum of square errors, the algorithm can provide a good balance of three types of errors and the overall imaging performance can be optimized. This study is an important step toward a potential solution to quantitative image quality assessment.

$$\hat{m}(x,y) = \sum_{i=1}^{N} u_i(x,y)\,a_i(x,y) \quad (1)$$

$$a_i(x,y) = \sum_{j=0}^{R-1} d_i\left(x + \frac{jF_x}{R}, y\right) + n_i(x,y) \quad (2)$$

$$\hat{m}(x,y) - m(x,y) = e_1 + e_2 + e_3 \quad (3)$$

$$e_1(x,y) = \sum_{i=1}^{N} u_i(x,y)\,d_i(x,y) - m(x,y) \quad (4)$$

$$e_2(x,y) = \sum_{j=1}^{R-1}\sum_{i=1}^{N} u_i(x,y)\,d_i\left(x + \frac{jF_x}{R}, y\right) \quad (5)$$

$$e_3(x,y) = \sum_{i=1}^{N} u_i(x,y)\,n_i(x,y) \quad (6)$$

Theory: In general, the reconstruction of a set of 2D parallel imaging data can be represented as the weighted sum of acquired N-channel images in image space [3]. This relationship is shown in Eq. (1), where (x,y) is the 2D spatial coordinate, N is the channel number of a coil array, $\hat{m}(x,y)$ is the reconstructed image, $\{u_i(x,y), i=1, 2, \ldots, N\}$ represents the weighting coefficients for reconstruction and is referred to as "reconstruction operator" in this work, and $\{a_i(x,y), i=1,2,\ldots, N\}$ represents the acquired N-channel images, which may have aliasing due to undersampling in k-space. An acquired image from the ith (i=1,2,…,N) channel, $a_i(x,y)$, can be represented using the real ith-channel image $d_i(x,y)$ and the noise $n_i(x,y)$, as shown in Eq. (2), where R is the reduction factor in undersampling, and F_x is the FOV in phase encoding direction x. From Eqs. (1) and (2), one can derive Eq. (3). It can be seen that the difference between the reconstructed image $\hat{m}(x,y)$ and the object image $m(x,y)$ is the sum of three error components e_1, e_2, and e_3, which are given by Eqs. (4)-(6). Eq. (4) evaluates how well the real image intensity at position (x,y) is preserved in reconstruction and we refer to e_1 as "image fidelity error". Eq. (5) indicates whether the image aliasing from positions other than (x,y) would be totally removed and e_2 represents the residual aliasing artifacts. Eq. (6) describes how reconstruction operator amplifies the noise in the acquired images and e_3 represents the amplified noise. These three types of errors can be also understood as follows: Every reconstruction algorithm is based on a linear equation in the form of "**Ax=b**", where the vectors **x** and **b** are from the fully- and under-sampled data respectively, and **A** is a matrix related to coil sensitivities. Perfect reconstruction requires calculating a matrix **B** for reconstruction such that **BA** equals an identity matrix. The image fidelity error e_1 is generated from the "non-identity" of diagonal elements in **BA** and the residue aliasing artifacts e_2 is from the "non-zero" of non-diagonal elements in **BA**. The power gain in the matrix **B** may amplify the noise in reconstruction and is the cause of amplified noise e_3. Different reconstruction algorithms minimize different combinations of three types of errors. For quantitative assessment, one can use Eqs. (4)-(6) to separate the mixed effects of three types of errors on the image quality. To optimize reconstruction, we propose to minimize the weighted sum of square errors $\|e_1\|^2 + \alpha\|e_2\|^2 + \beta\|e_3\|^2$, where α and β are the relative weightings on aliasing artifacts and amplified noise with respect to that on data fidelity error.

Methods and Materials: Practically in parallel imaging, the real images $d_i(x,y)$'s and $m(x,y)$ are not available. The reconstruction operator can be calculated from a set of fully sampled low-resolution calibration data, which is either from pre-scan or from auto-calibration signals (ACS). The calibration data has high SNR. We can use this set of high SNR calibration data to approximate the noise-free images $d_i(x,y)$'s and $m(x,y)$ in the above equations. This will give a practical representation of three types of errors. The use of weighting parameters (α,β) allows the suppression of image fidelity error, aliasing artifacts, and noise to different degrees in reconstruction. The reconstruction operator can be calculated either in image space or in k-space. In k-space, the multiplication in above equations will become the convolution. The k-space data of images $d_i(x+jF_x/R,y)$'s for $j\neq0$ can be calculated by applying a linear phase adjustment to the calibration data in k-space. In this work, the proposed model was investigated using a set of brain imaging data acquired from an 8-channel coil array on a 3T clinical MRI scanner. A set of axial images was acquired with full Fourier encoding using a T_1 FLAIR sequence (FOV 220×220 mm, matrix size 512×512, TR 3060 ms, TE 126 ms, flip angle 90°, slice thickness 5 mm, number of averages 1). The phase encoding direction was left-right. The noise data for the calculation of amplified noise is acquired from a noise scan.

Results and Discussion: As an example, we investigated a k-space reconstruction method based on the proposed model using the brain imaging data. The acquired data was manually undersampled by a factor of 4. In calibration, 24 ACS lines were used. The 3D plot in Fig. 1 shows how the weighting parameters (α,β) affect the total reconstruction error with respect to the reference image in Fig. 2(a). Three regions of high error in Fig. 1 are marked with "F", "A" and "N". These letters represent three types of errors: image fidelity error (F), residual aliasing noise (A), and amplified noise (N). As shown in Figs. 2(b), (c), and (d), only one type of error is dominant in each of the regions F, A, and N and the patterns of three types of errors are different. The letter "B" in Fig. 1 indicates the region where three types of errors are well balanced using properly selected weighting parameters (α,β) and the total error is minimized. From the comparison of zoomed-in images in Fig. 2(e), (f) and (g), it can be seen that the reconstructed image in region B is less noisy than GRAPPA image, which drops in N region of Fig. 1. However, it should be understood that the best reconstruction for a particular application is not necessary to be in B region, where the total reconstruction error is lowest. Different application has different requirements for image fidelity error, aliasing artifacts, and noise level. The freedom in selecting weighting coefficients (α,β) in a reconstruction algorithm offers the possibility to optimize the reconstruction for different requirements. Practically, it is also usual that the data acquired from different imaging experiments contains different percentage of real image information, aliasing, and noise. The techniques based on the proposed mathematical model offer the advantage in suppressing three different types of errors based on the composition of actual datasets. Further work will focus on how each type of reconstruction error affects the imaging quality in the sense of clinical significance.

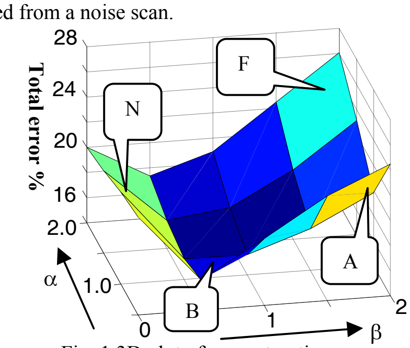

Fig. 1 3D plot of reconstruction error against weighting parameters α and β.

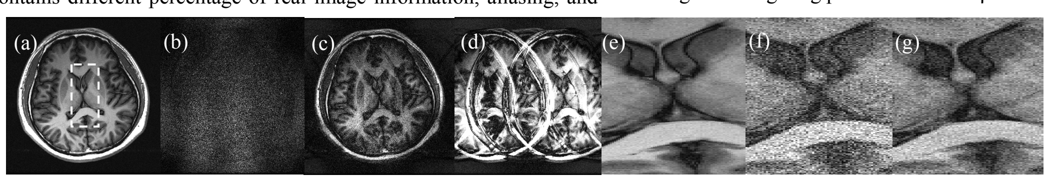

Fig. 2 (a) Reference image reconstructed from the full k-space data. (b) Error pattern in N region. (c) Error pattern in F region. (d) Error pattern in A region. (e), (f) and (g) are zoomed-in images inside the rectangular box in (a). (e) Reference image. (f) Reconstructed image using GRAPPA. (g) Reconstructed image in B region based on the proposed model. The reconstruction error of (g) (15.78%) is much less than that in (f) (21.94%).

Reference: [1]. Prussmann, K.P. et. al., MRM 1999, 42: 952-962. [2]. Griswold, M. A. et. al., MRM 2002, 47:1202-1210. [3]. Li Y. et al., IEEE TMI 2009, 28: 687-695.